frontiers | Frontiers in Marine Science

TYPE Original Research
PUBLISHED 05 September 2022
DOI 10.3389/fmars.2022.971648

OPEN ACCESS

EDITED BY
Hongyu Ma,
Shantou University, China

REVIEWED BY
Huan Wang,
Ningbo University, China
Yin Zhang,
Shantou University, China

*CORRESPONDENCE
Xiaowan Ma
bowl_88@hotmail.com

†These authors have contributed equally to this work

SPECIALTY SECTION
This article was submitted to Aquatic Physiology, a section of the journal Frontiers in Marine Science

RECEIVED 06 July 2022
ACCEPTED 10 August 2022
PUBLISHED 05 September 2022

CITATION
Qiao Y, Ma X, Huang L, Zhong S, Xing Y and Chen X (2022) Interaction analysis of hemolymph extracellular vesicles miRNA and hemocytes mRNA reveals genes and pathways associated with molting in *Scylla paramamosain*. *Front. Mar. Sci.* 9:971648. doi: 10.3389/fmars.2022.971648

Interaction analysis of hemolymph extracellular vesicles miRNA and hemocytes mRNA reveals genes and pathways associated with molting in *Scylla paramamosain*

Ying Qiao[1], Xiaowan Ma[1*†], Lixing Huang[2], Shengping Zhong[3†], Yongze Xing[1] and Xuyang Chen[1]

[1]Key Laboratory of Tropical Marine Ecosystem and Bioresource, Fourth Institute of Oceanography, Ministry of Natural Resources, Beihai, China, [2]Key Laboratory of Healthy Mariculture for the East China Sea, Ministry of Agriculture, Fisheries College, Jimei University, Xiamen, China, [3]Institute of marine drugs, Guangxi University of Chinese Medicine, Nanning, China

Molting is a key biological process in crustaceans, with impacts on their growth, development and reproduction. Extracellular vesicles (EVs) serve as bio-cargo carrying such as nucleic acids, proteins, and lipids which mediate intercellular communication and participate in various cell biological processes. In this study, we obtained hemocyte transcriptome data during the intermolt, premolt, and postmolt stages of the mud crab *Scylla paramamosain*. We analyzed the differentially expressed genes in the three stages of molt and identified a number of immune-related genes and structural cuticle genes. We then isolated and characterized the EVs from the hemolymph of *S. paramamosain* and sequenced their miRNA. In total, we characterized 89 EVs microRNAs (miRNAs) targeting 1447 genes that are potentially involved in the molting process of *S. paramamosain*. The EVs miRNAs mainly regulated the immune-related genes and affected the molting process by mediating ecdysone signaling and insulin signaling pathways during the mud crab molt cycle. This is the first study of EVs miRNAs and their interaction with mRNA to identify important candidate genes associated with, or regulating, the molting process. This study provides a better understanding of, and novel insights into, the molting cycle of crustaceans and offers baseline information for further studies in the mechanisms regulating molt.

KEYWORDS

extracellular vesicles (EVs), interaction analysis, molting, *Scylla paramamosain*, miRNA

Introduction

The mud crab *S. paramamosain*, inhabits estuaries and coastal waters in Southeast Asia and is one of the most economically important crustaceans in Chinese mariculture (Vay, 2001). Molting is a key biological process in the growth, development and reproduction of crustaceans (Chang and Mykles, 2011). Over the entire life cycle, *S. paramamosain* molt 18 times, including five developmental larval molts, several growth-related molts, and one last adult reproductive molt (Liu et al., 2021). Four major molt stages can be distinguished according to morphological features, including intermolt (InM), premolt (PrM), ecdysis (E) and postmolt (PoM) (Liu et al., 2021). The InM stage is the longest, and energy accumulates and muscles regenerate during this stage. Mud crabs generate a new exoskeleton during the PrM stage. The E stage is very short, taking from only a few seconds to a few minutes. During the E and PoM stages, the crab absorbs a large amount of water, expands its body, and hardens the new soft exoskeleton as quickly as possible (Chang and Mykles, 2011).

Molt is a precise procedure and is controlled by a complex multi-hormone system including ecdysone, the prohormone of the steroid molting hormone, and ecdysteroids, a class of steroid molting hormones (Gong et al., 2015). 20-hydroxyecdysone (20E) has been shown to be a physiologically active ecdysteroid (Gong et al., 2015). Other hormones, such as insulin and juvenile hormone, are also involved in the molting process (Song and Zhou, 2020; Yuan et al., 2020). Crustacean eyestalks are considered to constitute the molt control center and contain the X-organ/sinus gland (XO/SG) complex, which releases a number of peptide hormones such as molt-inhibiting hormone and crustacean hyperglycemic hormone into the hemolymph (Mykles, 2021). The hepatopancreas plays a vital role in energy storage and breakdown, nutrient accumulation, and carbohydrate and lipid metabolism during molt (Xu et al., 2020). Other core genes also participate in the molting process, such as those coding for ecdysone receptor (EcR) (Song et al., 2017), cuticle-related enzymes (chitinases, chitin deacetylase, and chitin synthase) (Zhou et al., 2018), and the structural proteins of the cuticle (Strus et al., 2015). The open circulatory system of crustaceans carries the hemolymph, which contains the hemocytes, oxygen, hormones, and nutrients, *etc*. The concentration of ecdysteroid in the hemolymph fluctuates dramatically during the molt cycle (Chang and Mykles, 2011). Thus, in addition to the XO-SG complex, the roles of the hemolymph and its contents should be borne in mind when considering the mud crab molting process.

Previously, researches on the molt of mud crabs have mainly focused on the effects of environmental factors on the molting process, endocrine regulation, and functional gene expression levels during the molt cycle (Abehsera et al., 2018; González et al., 2020; Minh Nhut et al., 2020; Abehsera et al., 2021). In addition, several reports of the transcriptomes of different crustacean tissues during molting cycle have been published, such as the gills (Li et al., 2019), eyestalks (Lv et al., 2017), hepatopancreas (Xu et al., 2020; Su et al., 2021), and muscles (Tian and Jiao, 2019). Moreover, the proteomes of the hepatopancreas of mud crabs during the molting cycle have also been reported (Liu et al., 2021). microRNAs (miRNAs) are small non-coding RNAs (18–25 nucleotides in length) which can bind to the 3' untranslated region (3'UTR) of target mRNAs and regulate the target genes. miRNAs are considered to play various important roles in many fundamental biological processes in animals, including cell differentiation, proliferation, development, apoptosis, metabolism, signal transduction, immunity, and evolution (Saliminejad et al., 2019). Some studies have investigated the roles of miRNAs in *S. paramamosain*, including miRNA modulation of networks underlying osmoregulation (Wang et al., 2018) and WSSV infection (Lai et al., 2020). However, there is a lack of information on the miRNAs modulation during molting cycles of mud crab. Combining information on the mRNAs and protein profiles will better explain the complex biological processes of molting at the miRNA level.

Extracellular vesicles (EVs) are endocytic in origin, produced by various donor cells and released into the extracellular environment (Kalluri and LeBleu, 2020). They serve as mediators in intercellular communications and transport bio-cargoes, including lipids, proteins, mRNAs, and miRNAs. Numerous studies have shown that EVs are involved in multiple biological and pathological processes, such as reproduction and development, cancer progression, cardiovascular diseases, pathogen infection, and immune responses (Kalluri and LeBleu, 2020). miRNAs can be packaged into EVs to modulate the expression of specific target genes in recipient cells (Bartel, 2004). Recent studies on mud crabs have demonstrated the novel role of exosome miRNAs after viral infection and clarified the mechanisms underlying exosome-mediated apoptosis during the innate immune response (Gong et al., 2020; Gong et al., 2021). However, little information was known regarding the function of EVs miRNAs during the molt process.

In recent years, the study of EVs and the development of miRNAs high-throughput sequencing technology have provided new ideas for the study of the molting process of mud crabs. This study isolated and characterized the EVs in the hemolymph of *S. paramamosain* and characterized the EVs miRNAs and the target genes potentially involved in *S. paramamosain* molt. This is the first study of EVs miRNAs and their interactions with mRNA to identify important candidate genes associated with, or playing regulatory roles in, the molting process. This work provides novel insights into the molt cycle of *S. paramamosain*, and contributes to a better understanding of it. It provides a basic resource for further studies into the mechanisms regulating molt.

Materials and method

Sample collection

Healthy mud crabs (weighing 300 ± 11.2 g) were captured at random from a local crab farm (Beihai, Guangxi, China). Prior to the experiment, crabs were cultured for a week in 0.5 t plastic tanks before sampling, to acclimate to laboratory conditions (25‰ salinity, temperature 28°C). Three molt stages were identified based on morphological features: PoM, InM, and PrM. Three individuals from each stage were sampled. Hemolymph samples were collected using 5 mL syringes containing 1 mL EDTA (Solarbio, Beijing, China) and centrifuged at 500 × g for 5 min to collect the supernatant and hemocytes. All the samples were immediately frozen in liquid nitrogen for storage. The mud crabs were processed according to the Guidelines for the Ethical Review of Laboratory Animal Welfare, People's Republic of China National Standard GB/T 35892-2018.

mRNA sequencing and analysis

Total RNA was extracted from the mud crab hemocytes using a PureLink RNA Mini Kit (Ambion, California, USA) according to the manufacturer's protocols. RNA integrity was tested using an Agilent 2100 Bioanalyzer (Agilent Technologies, Palo Alto USA). Samples with a RIN ≥ 7 were used to construct libraries using a TruSeq Stranded mRNA LTSample Preparation Kit (Illumina, San Diego, USA). Transcriptome sequencing was then performed by OE Biotech Co., Ltd. (Shanghai, China) on an Illumina platform HiSeq 2500.

Raw reads containing ploy-N and low-quality reads were removed to obtain clean reads. Unigenes were annotated using a variety of databases: NCBI nonredundant (NR), SwissProt, Clusters of orthologous groups for eukaryotic complete genomes (KOG), the Gene ontology (GO) classification, and the Kyoto Encyclopedia of Genes and Genomes (KEGG). The fragments per kilobase million (FPKM) of each unigene was calculated using bowtie2 and eXpress. Differentially expressed genes (DEGs) were identified using DESeq (https://bioconductor.org/packages/release/bioc/html/DESeq2.html), in which unigenes with a threshold P value < 0.05 and foldChange > 2, or foldChange < 0.5 were considered to be significantly differentially expressed. Heatmap and principal component analyses (PCA) were conducted using R version 3.5.2 (https://cran.r-project.org/bin/windows/base/old/3.5.2/). Venn diagrams were drawn using the Venny 2.1 program (http://bioinfogp.cnb.csic.es/tools/venny/).

Isolation and analysis of EVs

Mud crab EVs were isolated from 10 mL hemolymph samples taken from three individuals from each molt stage and separated to collect the supernatants. The supernatants were centrifuged at 10,000 × g for 30 min to remove cell debris, filtered (pore size 0.22 μm), and subjected to ultracentrifugation (Beckman, Optima XE, Duarte, USA) at 120,000 × g for another 70 min. The resulting EVs pellets were resuspended in 200 μl DEPC PBS.

A NanoSight NS300 (Malvern Instruments Ltd, Malvern, UK) was used to quantify EVs and to generate EVs size distribution profiles. The EVs were also imaged using a JEOL JEM-1230 transmission electron microscope (JEOL, Tokyo, Japan). The mud crab EVs were characterized using three phylogenetically conserved EVs markers: CD81 (diluted 1:500), HSP70 (diluted 1:2000), and TSG101 (diluted 1:1000). Calnexin (diluted 1:2000) and GAPDH (diluted 1:10,000) were used as negative controls.

EVs miRNA sequencing and analysis

miRNA was extracted from EVs using a mirVana miRNA Isolation Kit and sequenced by OE biotech Co., Ltd. (Shanghai, China). Low-quality reads, reads with 5' primer contaminants, poly (A) reads, reads without 3' adapters and insert tags, and reads shorter than 15 nt and longer than 41 nt, were all filtered from the raw data. Known miRNAs were identified using the miRBase v21 database (http://www.mirbase.org/) and novel miRNAs were predicted using mirdeep2 v2.0.0.8 (http://www.mirbase.org/). Differentially expressed miRNAs with P < 0.05 were identified, calculated using the DEG algorithm in the R package. The target genes of differentially expressed miRNAs were predicted using the miRanda software (http://www.microrna.org/). GO enrichment and KEGG pathway enrichment analysis of differentially expressed miRNA target genes were performed using R. The interactions between miRNA and target genes were visualized using Cytoscape_3.3 (https://cytoscape.org/download.html).

Results

De novo assembly and functional annotation of the mRNA transcriptomes of hemocytes in the three molt stages of *S. paramamosain*

The transcriptome data were obtained from the mud crab hemocytes in the InM (Figure 1A), PrM (Figure 1B), and PoM stages (Figure 1C). A total of 62.33 G clean reads with an average length of 1362.17 bp were generated (Supplementary Table 1). The original sequencing data were uploaded to the NCBI BioProject database with accession number: PRJNA842705.

FIGURE 1
Three molt stages of *S. paramamosain*. **(A)** intermolt (InM, all parts of the body were hard). **(B)** premolt (PrM, the old and new carapaces were separated completely). **(C)** postmolt (PoM, parts of the body were flaccid).

The assembled unigenes were searched against the NCBI, NR, KEGG, SwissProt, KOG, GO, and Pfam databases, using BLAST + (E-value, 10^{-6}) (https://blast.ncbi.nlm.nih.gov/Blast.cgi?PAGE_TYPE=BlastDocs&DOC_TYPE=Download). Of the 31,713 assembled unigenes: 14,921 (47.05%) were annotated to NR; 9,376 (29.57%) to SwissProt; 4,225 (13.32%) to KEGG; 8,265 (26.06%) to KOG; 8,651 (27.28%) to GO; and 8,833 (27.85%) to Pfam.

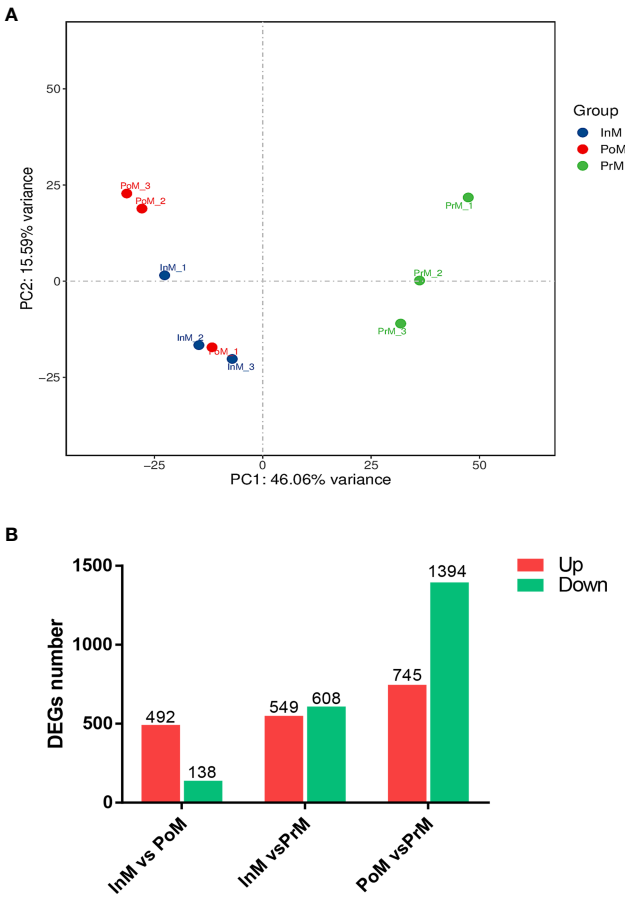

FIGURE 2
mRNA expression overview of molt stages of *S. paramamosain*. **(A)** PCA analysis between adjacent molting stages in *S. paramamosain*. **(B)** Differentially expressed genes between adjacent molting stages in *S. paramamosain*. The values in red and green indicate the numbers of upregulated and downregulated mRNA. PoM, postmolt; InM, intermolt; PrM, premolt.

Analysis of the DEGs in the hemocytes of the three molt stages of *S. paramamosain*

Based on similarities in gene expression patterns, all of the DEGs in the samples could be clustered into three groups, as shown by the PCA plot (Figure 2A). Pairwise comparisons of gene expression were made between consecutive molt stages to gain insight into global gene expression levels in the hemocytes during molt. The analysis of the DEGs showed that a total of 630 unigenes were differentially expressed between the InM and PoM stages, of which 492 were upregulated and 138 were downregulated. A total of 2139 unigenes were differentially expressed between the PoM and PrM stages (745 upregulated and 1394 downregulated). A total of 1157 unigenes, were differentially expressed between the PrM and InM stages (608 upregulated and 549 downregulated) (Figure 2B).

Of the DEGs, 37 unigenes were differentially expressed in all three molt stages InM vs PoM, PoM vs PrM, and InM vs PrM, including the cuticle proteins and several hormone-related genes (Figure 3). 445 unigenes were only differentially expressed between InM and PoM stages, including insect cuticle protein, broad-complex core protein, prophenoloxidase (proPO), and crustin (Figure 3). 468 genes were only differentially expressed between the PrM and InM stages, including several exoskeleton-related genes such as Di-N-acetylchitobiase, chitinase domain-containing protein, and dynein heavy chain. Between the PoM and PrM stages, 765 shared DEGs were detected, notably those related to immunity and exoskeleton-related genes (Figure 3). In addition, we found 560 DEGs only at the intersections of PoM vs PrM and InM vs PrM, including exoskeleton-related genes (chitin binding-like protein, cuticle protein, early cuticle protein, *etc.*) and immune-related genes (inhibitor of apoptosis protein, scygonain, *etc.*) (Figure 3).

Of the DEGs, several immune related genes were discovered, such as antimicrobial peptides (AMPs), genes involved in the Toll pathways and proPO cascades (Supplementary Table 4 and Figure 3). The AMPs of crustin were significantly upregulated at the InM stage, and the scygonadin was upregulated at the PrM stage. The proPO transcripts were upregulated in the InM and PrM stages. The genes involved in the Toll pathway (clip domain serine proteinase, mannnose-binding lectin, and Serine protease 55) were all significantly upregulated in the InM stage. In the PrM stage, most of the Toll pathways genes were upregulated (Pro-resilin-like, inhibitor of apoptosis protein, FAS-associated factor 1-like) with the exception of Serine protease 55. Besides the immune related genes, we also discovered a bunch of genes involved in the cuticle formation and these genes were the most actively expressed in the PrM stage (Supplementary Table 4 and Figure 3).

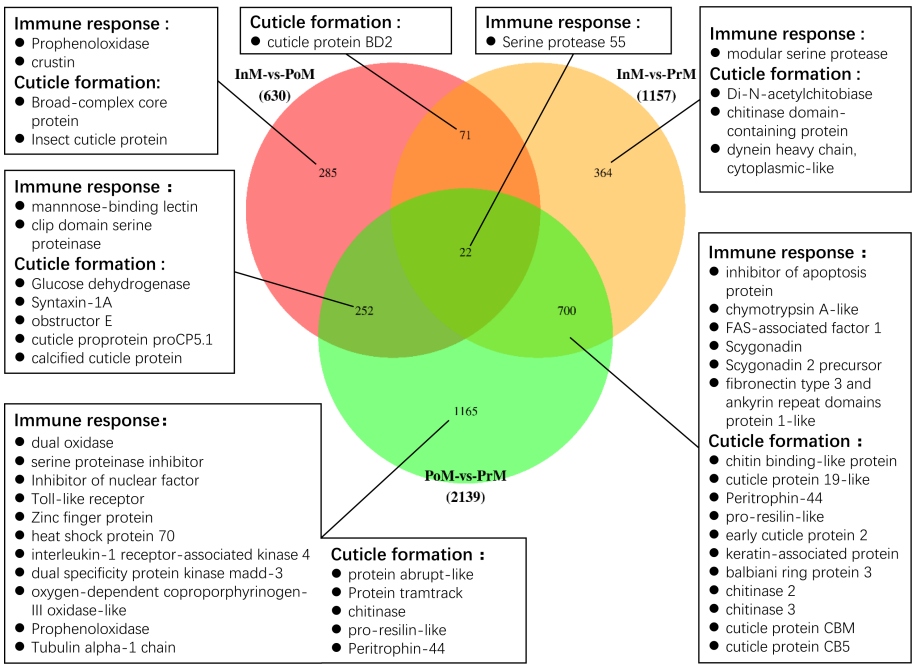

FIGURE 3
Venn diagram of the DEGs among three molting stages. The numbers of the unique and common DEGs are indicated. The genes related to immune response and cuticle formation have been listed.

GO and KEGG analysis of the DEGs of hemocytes in the three molt stages of *S. paramamosain*

The DEGs were related to the GO and KEGG databases to obtain complete functional information classifying the molting process of mud crabs. GO analysis revealed that the upregulated DEGs of the InM vs PoM stages were mostly enriched in the molecular functions relating to serine-type endopeptidase activity and the biological processes involved in innate immune responses. The downregulated DEGs of the InM vs PoM stages were mostly enriched in molecular functions related to the structural constituents of the cuticle and the biological process of RNA polyadenylation. In the molecular function category between the InM and PrM stages, a large number of upregulated DEGs were associated with polysaccharide binding, and the downregulated DEGs were involved in serine-type endopeptidase activity. Within the biological processes between the InM and PrM stages, upregulated DEGs were mostly enriched in defense responses to fungus attacks, and the downregulated DEGs were associated with the carnitine biosynthetic process. In the analysis of the PoM vs PrM stages, the largest cluster of upregulated DEGs was associated with the biological process category of positive regulation of inflammatory response and the molecular function of polysaccharide binding. Meanwhile, the biological process category innate immune response and the molecular function serine-type endopeptidase activity were the most abundant categories among the downregulated DEGs (Figure 4A).

In the KEGG pathway analysis of DEGs between the InM and PoM stages, the top five were enriched in Riboflavin metabolism, Prion diseases, Arginine and proline metabolism, Glycolysis/

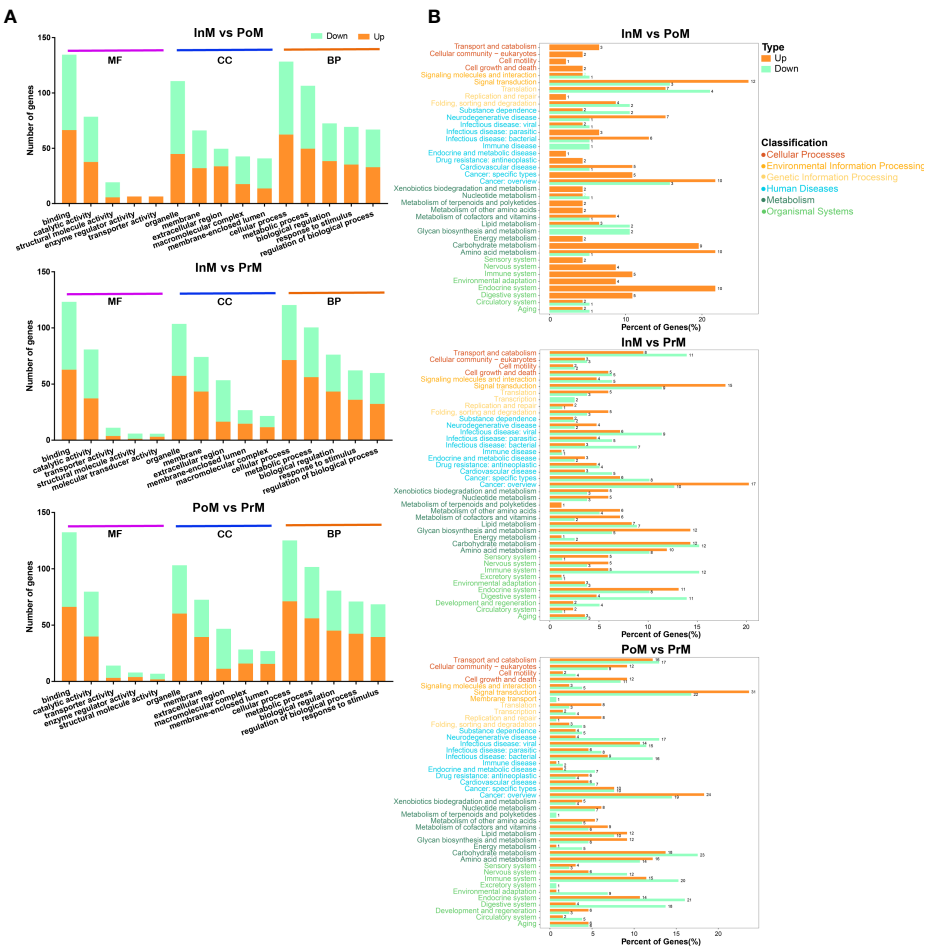

FIGURE 4
Enrichment of DEGs between the molting stages in GO and KEGG annotation. **(A)** Enriched GO terms of DEGs between the molting stages. MF, Molecular Function; CC, cellular component; BP, biological process. **(B)** KEGG enrichment analysis of DEGs between the molting stages. PoM, postmolt; InM, intermolt; PrM, premolt.

Gluconeogenesis, and Arginine biosynthesis. The top five KEGG pathways for DEGs between the InM and PrM stages were enriched in Neuroactive ligand-receptor interaction, Glycolysis/Gluconeogenesis, Chemical carcinogenesis, Glycosphingolipid biosynthesis-globo and isoglobo series, and Complement and coagulation cascades. The top five KEGG pathways of DEGs between the InM and PoM stages were enriched in Complement and coagulation cascades, Glycolysis/Gluconeogenesis, Other glycan degradation, Glycosphingolipid biosynthesis-globo and isoglobo series, and Lysosome (Figure 4B).

The involvement of EVs in the molting process of mud crabs

To characterize the EVs of mud crabs during the molting process, we isolated EVs from the hemolymph of the InM, PrM, and PoM stages. The cup-shaped structure and size of the isolated EVs were detected using a transmission electron microscope (Figure 5A) and nanoparticle tracking analysis (NTA) (Figure 5B). Three exosome markers (CD81, HSP70, and TSG010) were detected using western blot to further ascertain that the isolated particles were in fact EVs (Figure 5C).

EVs miRNA expression profiling in the molting process of mud crabs

The miRNA profiles of EVs in the InM, PrM, and PoM stages were sequenced (Supplementary Table 2) and 329.95 M raw reads were obtained. To understand and illustrate the relationship between InM, PoM and PrM, we performed hierarchical clustering of the DE miRNAs from all the samples (Figure 6 A) After removing sequences less than 15 nt or longer than 41 nt (Figure 6B), reads with Q20 less than 80%, and those containing N bases, 171.11 M reads were obtained. To characterize the miRNAs, all of the sequences were compared in the miRbase 22.0 database to discover known miRNAs. A total of 379 miRNAs were identified as previously known. The original sequencing data were uploaded to the NCBI BioProject database with accession number: PRJNA842845.

A total of 61 EVs miRNAs were differentially expressed between the InM and PrM stages (42 upregulated and 19 downregulated), using the criteria of at least a 2-fold difference and a $P < 0.05$. In addition, 65 differentially expressed miRNAs were expressed comparing PoM and InM. Among them, 44 were upregulated and 21 downregulated. Comparing InM and PoM, 24 EVs miRNAs were differentially expressed, 10 upregulated and 14 downregulated (Figures 6C, D).

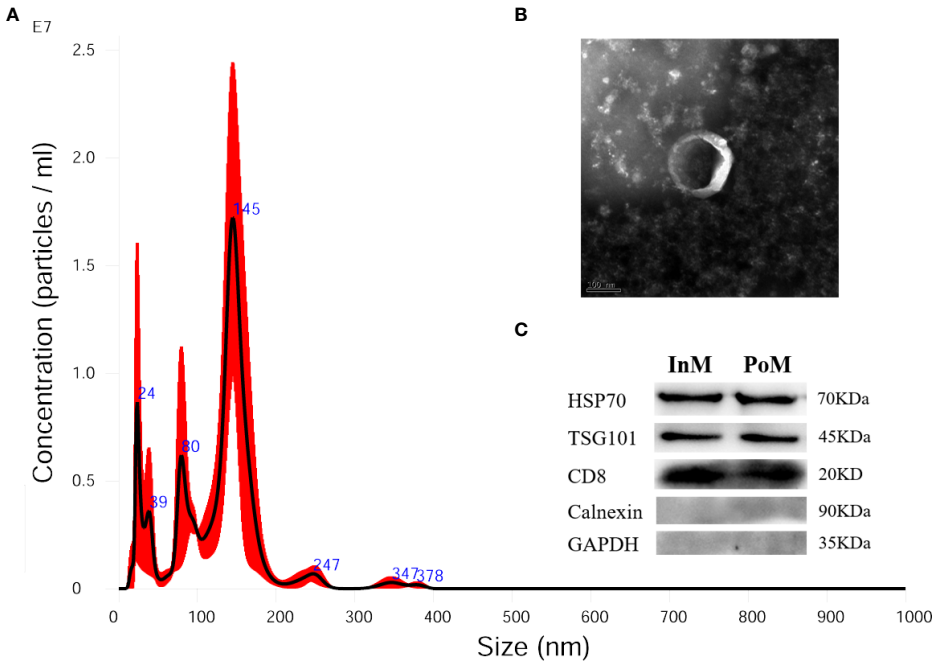

FIGURE 5
Isolated EVs from hemolymph of *S. paramamosain*. **(A)** Nanoparticle tracking analysis (NTA) showing a representative size distribution profile of mud crab EVs. **(B)** Transmission electron microscopy (TEM) from mud crab EVs; scale bar represents 100 nm. **(C)** Western blotting analysis (WB) showing mud crab EVs positive for CD81, HSP70 and TSG101; Calnexin and GAPDH served as negative control; the molecular weight for standard is indicated in kilodaltons (kDa).

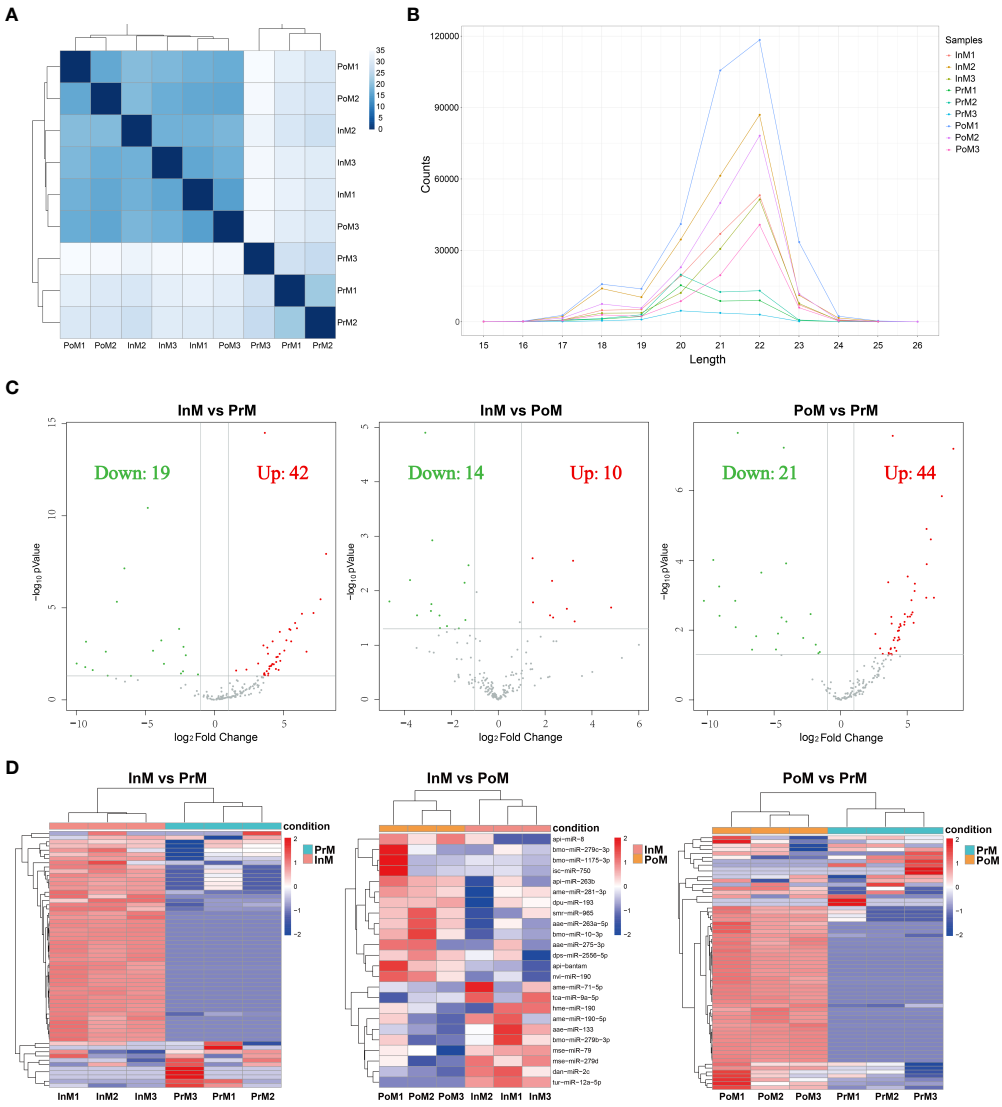

FIGURE 6
Annotation and analysis of mRNAs. **(A)** The DE miRNAs correlation heatmap of sample clustering. **(B)** Length distribution of miRNAs. **(C)** Volcano plot of the DE miRNAs between adjacent molting stages of *S. paramamosain*. The horizontal axis shows the $\log_2$ Fold change, and the vertical axis represents -$\log_{10}$ pvalue. The grey color represents the unchanged, red color represents upregulated, and the green color represents the downregulated DE miRNAs. PoM, postmolt; InM, intermolt; PrM, premolt. **(D)** Heatmap diagram of the DE miRNAs between adjacent molting stages of *S. paramamosain*. Each row represents one miRNA. The horizontal axis represents the sample clusters. Each column represents one biological replicate. The red and blue segments indicate relatively high and low expression level. PoM, postmolt; InM, intermolt; PrM, premolt.

Bioinformatics analysis of EVs miRNA target genes and functional enrichment analysis of miRNA target genes and pathways

RNAhybrid (v2.1.2) (x) + svm_light (v6.01) (x), Miranda (v3.3a) (x), and TargetScan (v7.0) (x) were used to predict target genes. The intersection of the results of these three methods were considered as miRNA-target genes. A total of 89 EVs miRNAs targeting 1447 genes were predicted, covering a wide range of functions (Supplementary Table 3).

GO analysis showed that miRNA-target genes were considerably enriched in the GO terms of biological processes (Figure 7A) (*e.g.*, ubiquitin-dependent protein catabolic process, positive regulation of transcription by RNA polymerase II, and negative regulation of apoptotic process), cell components (*e.g.*, cytoplasm, nucleus, and cytosol), and molecular function (*e.g.*, metal ion binding, ATP binding, and DNA binding).

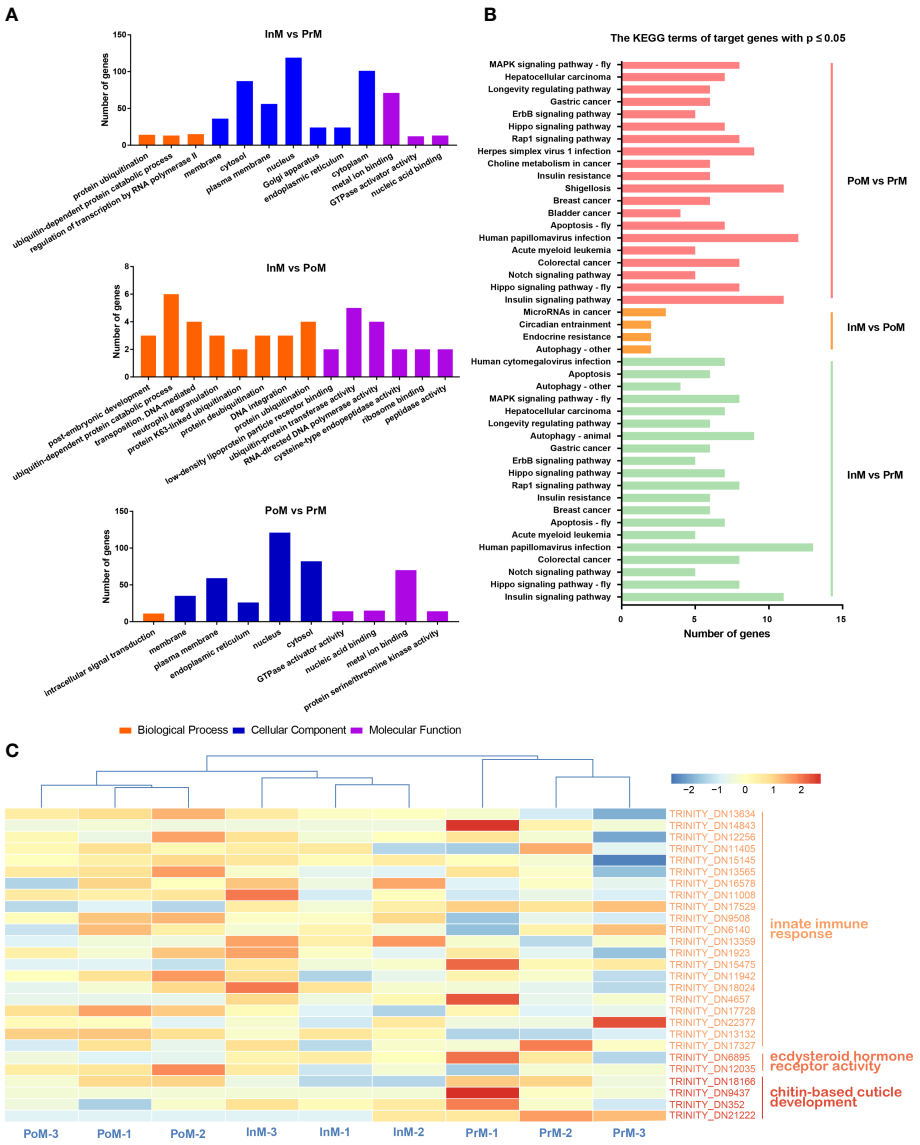

FIGURE 7
Functional enrichment analysis of miRNA target genes and pathways. **(A)** GO enrichment analysis of miRNA target genes. **(B)** KEGG enrichment analysis of the miRNA target genes between adjacent molting stages of *S. paramamosain*. PoM, postmolt; InM, intermolt; PrM, premolt. **(C)** Heatmap of miRNA target genes involved in innate immune response, ecdysteroid hormone receptor activity and chitin-base cuticle development in molting stages in *S. paramamosain*. Colored keys represent the $\log_{10}$(FPKM+1) of target genes between adjacent molt stages. The red color represents upregulation and the blue color represents downregulation. Each column represents one biological replicate and each row represents a miRNA target gene.

KEGG enrichment analysis showed that the 1447 predicted putative target genes were grouped into 238 KEGG terms (Figure 7B). Among these pathways, the Insulin signaling pathway, Hippo signaling pathway, Notch signaling pathway, Colorectal cancer, and Human papillomavirus infection were the five main pathways in the InM vs PrM comparison. Insulin signaling pathway, Hippo signaling pathway, Notch signaling pathway, Colorectal cancer, and Acute myeloid leukemia were the top five pathways in PoM vs PrM. Between InM vs PoM, the most enriched pathways were Autophagy-other, Endocrine resistance, Circadian entrainment, and MicroRNAs in cancer.

In addition, we identified several target genes related to innate immune response, ecdysteroid hormone receptor activity, and chitin-based cuticle development (Figure 7C and Table 1), including tumor necrosis factor, anti-lipopolysaccharide factor (ALF), dual oxidase 1, EcR, and ecdysone-induced protein 74EF (Eip74EF).

TABLE 1 EVs miRNAs with putative target genes in relation to innate immune response, ecdysteroid hormone receptor activity, and chitin-based cuticle development.

miRNA ID	Target genes ID	NR ID	NR annotation
miR-34	TRINITY_DN13634	MPC18128.1	Zinc finger E-box-binding homeobox protein zag-1
miR-133	TRINITY_DN14843	AWK27045.1	X-linked inhibitor of apoptosis protein
miR-2556	TRINITY_DN12256	XP_027239479.1	uncharacterized protein LOC113830469
miR-6056	TRINITY_DN11405	AYD41594.1	tumor necrosis factor, partial
miR-307	TRINITY_DN15145	SLM84439.1	Toll-like receptor 2
miR-282	TRINITY_DN13565	AVN99055.1	SRSF protein kinase 3-like, partial
miR-34	TRINITY_DN16578	MPC54724.1	Serine proteinase stubble
miR-184	TRINITY_DN11008	AJR22372.1	serine proteinase inhibitor-2
miR-14	TRINITY_DN17529	MPC29207.1	Serine protease 44
miR-34	TRINITY_DN9508	MPC36616.1	Peptidyl-prolyl cis-trans isomerase
miR-6056	TRINITY_DN6140	QCU71416.1	Nuclear factor interleukin 3-regulated transcription factor
miR-14	TRINITY_DN13359	AQV03739.1	i-type lysozyme
miR-34	TRINITY_DN1923	ROT68746.1	hypothetical protein C7M84_013112
miR-34	TRINITY_DN15475	AVN99053.1	glycogen phosphorylase, partial
miR-34	TRINITY_DN11942	MPC20397.1	Germinal-center associated nuclear protein
miR-995	TRINITY_DN18024	XP_027228265.1	fibrocystin-L-like
miR-92	TRINITY_DN4657	AXN93677.1	dual oxidase 1
miR-375	TRINITY_DN17728	XP_027229017.1	DNA mismatch repair protein Msh2-like
miR-6016	TRINITY_DN22377	AHK59786.1	C-type lectin
miR-34	TRINITY_DN13132	AHB62419.1	anti-lipopolysaccharide factor
miR-34	TRINITY_DN17327	AYV97198.1	alpha-2 macroglobulin
miR-34	TRINITY_DN6895	AGB34182.1	ecdysone receptor isoform 2a
miR-14	TRINITY_DN12035	XP_027206747.1	ecdysone-induced protein 74EF-like
miR-34	TRINITY_DN18166	XP_027209046.1	dynein heavy chain, cytoplasmic-like
miR-34	TRINITY_DN9437	XP_027228021.1	uncharacterized protein LOC113819973
miR-2	TRINITY_DN352	XP_027217714.1	uncharacterized protein LOC113810207
miR-6056	TRINITY_DN21222	MPC32089.1	Chondroitin proteoglycan 2

Interaction analysis of EVs miRNAs and hemocyte mRNAs in the molting process of mud crabs

To further explore the potential network of miRNAs and mRNAs, the interaction networks of miRNAs-mRNAs were constructed based on the DEGs of hemocytes and differentially expressed EVs miRNAs (Figure 8 and Table 2). In total, 50 pairs of differentially expressed miRNAs and mRNAs displaying negative correlations were found. In most cases, the miRNAs were found to target only one mRNA, such as miR-1175 targeting nitric oxide synthase, and miR-278 targeting Retrovirus-related Pol polyprotein from type-2 retrotransposable element R2DM. It was also found that a single differentially expressed miRNA could participate in the regulation of multiple DEGs. For example, miR-34 had 15 target mRNAs, and miR-6056 had seven target genes.

Discussion

Molting is one of the most essential events in the growth and development of S. paramamosain. The hemolymph of mud crabs circulates in an open circulatory system and plays an important role in facilitating the molt process. EVs carry nucleic acids around the body (Kalluri and LeBleu, 2020) and participate in various aspects of cell biology (Kalluri and LeBleu, 2020). To better understand the physiological regulation of molt, it is vital to identify the transcriptional regulatory genes and EVs miRNAs associated with the molting process.

In this study, we found that most of the immune-related genes were upregulated at the InM and PrM stages in the hemocyte transcriptome data. The AMP of crustin was significantly upregulated at the InM stage. Crustins are cysteine-rich antibacterial peptides which are widely discovered in decapoda crustaceans with a broad spectrum of antibacterial activity (Rekha et al., 2018). This result

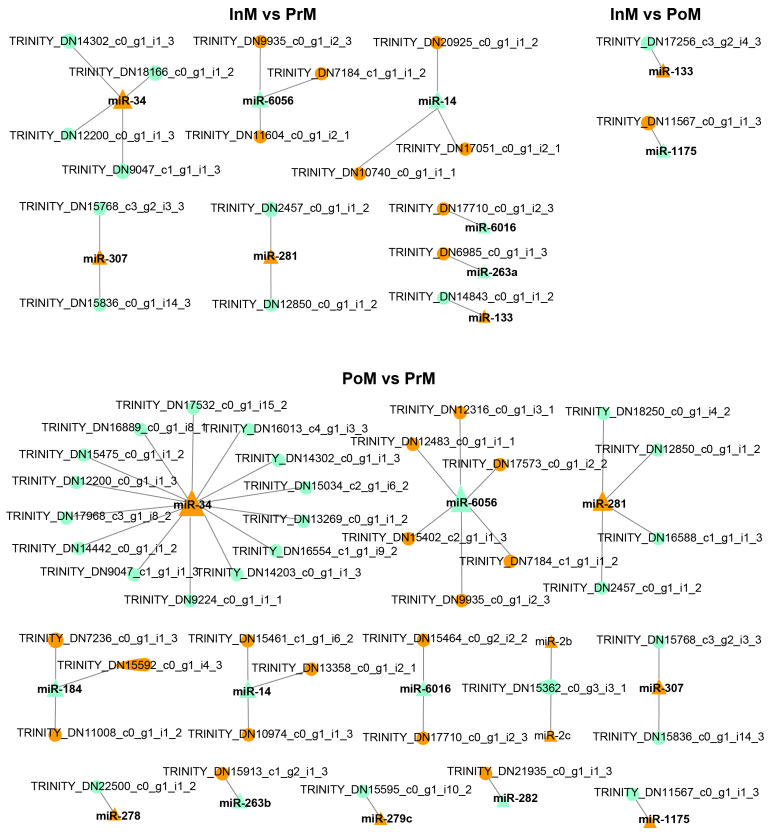

FIGURE 8
Interaction analysis of mRNA and EVs miRNAs. The triangles are miRNA, the circles are mRNA, orange color represents upregulated, and light green color represents downregulated, and the size represents connectivity.

TABLE 2 The interaction networks of EVs miRNAs and mRNAs in *S. paramamosain* molt stages.

miRNA id	Regulation	Gene id	log_2FC	p-value	Regulation	NR annotation
InM vs PoM						
miR-1175	Down	TRINITY_DN11567_c0_g1_i1_3	1.17	7.01E-06	Up	nitric oxide synthase
miR-133	Up	TRINITY_DN17256_c3_g2_i4_3	-2.40	0.000339	Down	Sacsin
InM vs PrM						
miR-6056	Down	TRINITY_DN11604_c0_g1_i2_1	2.73	0.000601	Up	Protein prune 2
miR-133	Up	TRINITY_DN14843_c0_g1_i1_2	-9.34	0.000529	Down	X-linked inhibitor of apoptosis protein
miR-6016	Down	TRINITY_DN17710_c0_g1_i2_3	3.26	1.31E-05	Up	WSC domain-containing protein 1
miR-14	Down	TRINITY_DN17051_c0_g1_i2_1	1.90	0.00011	Up	PREDICTED: prostaglandin E2 receptor EP4 subtype-like
miR-281	Up	TRINITY_DN12850_c0_g1_i1_2	-1.73	8.05E-05	Down	Mitochondrial carnitine/acylcarnitine carrier protein
miR-34	Up	TRINITY_DN9047_c1_g1_i1_3	-3.78	6.06E-05	Down	hypothetical protein C7M84_012357
miR-6056	Down	TRINITY_DN9935_c0_g1_i2_3	4.01	2.81E-08	Up	hypothetical protein
miR-281	Up	TRINITY_DN2457_c0_g1_i1_2	-1.60	0.000911	Down	hypothetical protein
miR-263	Down	TRINITY_DN6985_c0_g1_i1_3	2.33	0.000165	Up	hypothetical protein
miR-14	Down	TRINITY_DN20925_c0_g1_i1_2	6.25	0.000965	Up	hypothetical protein
miR-34	Up	TRINITY_DN14302_c0_g1_i1_3	-11.35	1.56E-13	Down	Four-domain proteases inhibitor
miR-34	Up	TRINITY_DN18166_c0_g1_i1_2	-1.05	0.000255	Down	dynein heavy chain, cytoplasmic-like

(Continued)

10.3389/fmars.2022.971648

TABLE 2 Continued

miRNA id	Regulation	Gene id	log_2FC	p-value	Regulation	NR annotation
miR-307	Up	TRINITY_DN15836_c0_g1_i14_3	-2.36	3.28E-06	Down	beta-actin
miR-6056	Down	TRINITY_DN7184_c1_g1_i1_2	2.73	6.04E-05	Up	–
miR-34	Up	TRINITY_DN12200_c0_g1_i1_3	-1.76	3.87E-10	Down	–
miR-307	Up	TRINITY_DN15768_c3_g2_i3_3	-3.95	4.44E-09	Down	–
miR-14	Down	TRINITY_DN10740_c0_g1_i1_1	3.68	0.00051	Up	–
PoM vs PrM						
miR-6016	Down	TRINITY_DN17710_c0_g1_i2_3	3.06	0.002804	Up	WSC domain-containing protein 1
miR-6016	Down	TRINITY_DN15464_c0_g2_i2_2	1.96	0.002464	Up	uncharacterized protein LOC113804112
miR-184	Down	TRINITY_DN15592_c0_g1_i4_3	1.61	0.000508	Up	transmembrane and coiled-coil domains protein 1-like isoform X2
miR-14	Down	TRINITY_DN13358_c0_g1_i2_1	1.11	0.00184	Up	transcription factor CSL
miR-34	Up	TRINITY_DN17532_c0_g1_i15_2	-1.68	0.001763	Down	serine/threonine-protein phosphatase 6 regulatory subunit 3-like isoform X2
miR-184	Down	TRINITY_DN11008_c0_g1_i1_2	2.02	0.000523	Up	serine proteinase inhibitor-2
miR-6056	Down	TRINITY_DN17573_c0_g1_i2_2	1.01	0.002449	Up	rho GTPase-activating protein 29-like
miR-278	Up	TRINITY_DN22500_c0_g1_i1_2	-5.65	0.001643	Down	Retrovirus-related Pol polyprotein from type-2 retrotransposable element R2DM
miR-34	Up	TRINITY_DN16889_c0_g1_i8_1	-2.38	3.48E-09	Down	putative RB13-6 antigen
miR-34	Up	TRINITY_DN15034_c2_g1_i6_2	-1.25	0.000187	Down	putative phosphatidylinositol 3-kinase catalytic subunit type 3 isoform X1
miR-14	Down	TRINITY_DN10974_c0_g1_i1_3	1.23	1.16E-06	Up	putative CCR4-NOT transcription complex subunit 6-like isoform X1
miR-34	Up	TRINITY_DN16554_c1_g1_i9_2	-1.24	0.000996	Down	Protein timeless
miR-6056	Down	TRINITY_DN12483_c0_g1_i1_1	1.20	0.00261	Up	Protein Shroom4
miR-34	Up	TRINITY_DN13269_c0_g1_i1_2	-2.70	9.22E-08	Down	Phosphatidylinositol transfer protein alpha isoform
miR-1175	Up	TRINITY_DN11567_c0_g1_i1_3	-2.10	7.90E-08	Down	nitric oxide synthase
miR-34	Up	TRINITY_DN14203_c0_g1_i1_3	-1.63	3.99E-07	Down	M-phase inducer phosphatase-like isoform X1
miR-281	Up	TRINITY_DN12850_c0_g1_i1_2	-1.49	3.42E-05	Down	Mitochondrial carnitine/acylcarnitine carrier protein
miR-34	Up	TRINITY_DN16013_c4_g1_i3_3	-2.84	9.58E-09	Down	membrane metallo-endopeptidase-like 1 isoform X5
miR-34	Up	TRINITY_DN9047_c1_g1_i1_3	-7.15	7.15E-14	Down	hypothetical protein C7M84_012357
miR-6056	Down	TRINITY_DN9935_c0_g1_i2_3	3.73	2.76E-06	Up	hypothetical protein
miR-34	Up	TRINITY_DN9224_c0_g1_i1_1	-2.26	5.91E-05	Down	hypothetical protein
miR-282	Down	TRINITY_DN21935_c0_g1_i1_3	1.65	0.000719	Up	hypothetical protein
miR-281	Up	TRINITY_DN2457_c0_g1_i1_2	-2.11	1.20E-06	Down	hypothetical protein
miR-281	Up	TRINITY_DN16588_c1_g1_i1_3	-2.56	0.000327	Down	hypothetical protein
miR-184	Down	TRINITY_DN7236_c0_g1_i1_3	1.56	0.000374	Up	hypothetical protein
miR-14	Down	TRINITY_DN15461_c1_g1_i6_2	1.96	0.000244	Up	hypothetical protein
miR-6056	Down	TRINITY_DN12316_c0_g1_i3_1	1.28	0.00014	Up	hormone receptor 96
miR-34	Up	TRINITY_DN15475_c0_g1_i1_2	-1.07	0.001777	Down	glycogen phosphorylase, partial
miR-34	Up	TRINITY_DN14302_c0_g1_i1_3	-9.61	7.69E-12	Down	Four-domain proteases inhibitor
miR-34	Up	TRINITY_DN17968_c3_g1_i8_2	-2.15	0.000903	Down	Endothelin-converting enzyme-like 1
miR-2c	Up	TRINITY_DN15362_c0_g3_i3_1	-4.03	0.000622	Down	Cell wall-associated hydrolase
miR-2b	Up	TRINITY_DN15362_c0_g3_i3_1	-4.03	0.000622	Down	Cell wall-associated hydrolase
miR-307	Up	TRINITY_DN15836_c0_g1_i14_3	-3.45	5.50E-13	Down	beta-actin
miR-263b	Down	TRINITY_DN15913_c1_g2_i1_3	6.19	0.0023	Up	Ankyrin repeat and SAM domain-containing protein 3
miR-6056	Down	TRINITY_DN15402_c2_g1_i1_3	1.16	0.000715	Up	probable Ras GTPase-activating protein
miR-281	Up	TRINITY_DN18250_c0_g1_i4_2	-1.78	0.003144	Down	kinase D-interacting substrate of 220 kDa B-like
miR-6056	Down	TRINITY_DN7184_c1_g1_i1_2	3.08	2.62E-06	Up	–
miR-34	Up	TRINITY_DN12200_c0_g1_i1_3	-1.67	4.90E-11	Down	–
miR-34	Up	TRINITY_DN14442_c0_g1_i1_2	-3.48	4.19E-07	Down	–
miR-307	Up	TRINITY_DN15768_c3_g2_i3_3	-5.22	1.60E-15	Down	–
miR-279c	Up	TRINITY_DN15595_c0_g1_i10_2	-1.72	0.001414	Down	–

was similar to that of three AMPs (crustins, *Sp*Hyastatin, and lysozyme), which were upregulated in the InM stage in the hepatopancreas cDNA library of *S. paramamosain* (Xu et al., 2020). However, the AMP of scygonadin was upregulated at the PrM stage. Scygonadin was originally considered as a male-specific anionic AMP in mud crabs (Wang et al., 2007). It may also play a role in the different developmental stages of *S. paramamosain* from embryogenesis to maturation (Xu et al., 2011). The induced expression of AMPs acted as a mechanism of innate prophylactic immunity in *Drosophila melanogaster* during molting (An et al., 2012). Furthermore, we discovered that the EVs miRNA miR-34 could target ALF. The first ALF isoform was identified in the amoebocytes of the horseshoe crabs *Tachypleus tridentatus* and *Limulus polyphemus* (Tanaka et al., 1982). It could bind to lipopolysaccharide (LPS) to inhibit the coagulation cascade (Sruthy and Philip, 2021). The proPO activation system is also an vital part of the immune system in crustaceans (Cerenius and Söderhäll, 2004). We discovered several proPO transcripts significantly upregulated in the InM and PrM stages, which suggested the involvement of the proPO system in the molting process of mud crabs. Toll pathway have been well studied for its importance in innate immunity (Lemaitre and Hoffmann, 2007). Plenty of work involving crucial components of Toll pathway have been conducted in *S. paramamosain* (Chen et al., 2018). In our study, we discovered that the genes involved in the Toll pathway were upregulated in the InM and PrM. The actively expressed genes of immune related genes suggested a stronger immune reaction in crabs requiring protection at InM stage and during active cuticle formation at the PrM stage. However, fewer immune related genes were identified at the PoM stage in present study.

In this study, the KEGG analysis of the target genes showed that the insulin signaling pathway was the most enriched pathway in the different stages of molt. Insulin signaling regulates growth rate and the steroid hormone 20E regulates the growth period (Yuan et al., 2020), and these are considered to be the two principle factors determining final body size in insects (Buhler et al., 2017; Yuan et al., 2020). 20E is the principal steroid hormone regulating molt and metamorphosis (Yoo et al., 2021). EcR binds with 20E and directs crustacean metamorphosis by triggering a transcriptional cascade (Yoo et al., 2021). Eip74EF acts at the top of these hierarchies to coordinate the induction of target genes (Sun et al., 2004). In our study, we explored the involvement of EVs during the molting process of mud crabs. We discovered that the miR-34 and miR-14 in the EVs might modulate the Eip74EF and EcR respectively during the various molt stages. Previous studies have shown that miR-14 directly targets the mRNA of EcR (Chen and Fu, 2021). miR-34 is highly conserved in insects and has been shown to interact with the 3' UTR of the Eip74EF mRNA through the predicted binding sites. miR-34 has been considered a key miRNA in the integration of age-associated physiology (Liu et al., 2012). Moreover, the results of our analysis of the miRNA-mRNA interactions, besides showing the presence of miR-14 and miR-34, showed that miR-281 was also related to EcR. It has been shown in *Bombyx mori* that the expression of miR-281 is suppressed by treatment with 20E and that miR-281 participates in developmental regulation through the suppression of EcR expression (Jiang et al., 2013). Our results showed that the miRNAs carried in the hemolymph EVs of *S. paramamosain* function in regulating the molting process not only through the insulin signaling pathway but also through ecdysone signaling during the mud crab molt cycle.

Conclusions

In conclusion, a stronger immune reaction at the susceptible PoM and InM stages of molt was found in order to protect mud crabs *S. paramamosain* from infection, and that cuticle formation genes were more active at the PrM stage. This is the first study of EVs miRNAs and their interactions with mRNAs to identify important candidate genes associated with, or which play, regulatory roles in the molting process. EVs miRNAs from the hemolymph of *S. paramamosain* mainly regulated the immune-related genes and were involved in the molting process through the mediation of the ecdysone signaling and insulin signaling pathways during the molt cycle.

Data availability statement

The datasets presented in this study can be found in online repositories. The names of the repository/repositories and accession number(s) can be found below: https://www.ncbi.nlm.nih.gov/genbank/, PRJNA842705; https://www.ncbi.nlm.nih.gov/genbank/, PRJNA842845.

Ethics statement

The animal study was reviewed and approved by ethics committee of Fourth Institute of Oceanography, Ministry of Natural Resources.

Author contributions

YQ and SZ contributed to conception and design of the study. XM, YX, and XC organized the database. LH performed the statistical analysis. XM and LH wrote the manuscript. All authors contributed to manuscript revision, read, and approved the submitted version.

Funding

This work was funded by the Youth Foundation of Guangxi Zhuang Autonomous Region (2021JJB150073); Innovation Driven Development Foundation of Guangxi (AD19245135 & AD19245161); the General Program of Guangxi Zhuang

Autonomous Region (Grant No. 2021GXNSFAA220030); China Postdoctoral Scientific Foundation (2021M701798); the Fund of Hainan Provincial Key Laboratory of Tropical Maricultural Technologies (Grant No. TMTOF202104); the Guangxi Key Laboratory of Beibu Gulf Marine Biodiversity Conservation, Beibu Gulf University (Grant No. 2022KA04); Scientific Research and Technology Development Program of Guangxi (Grant No. AB16380105), the National Modern Agricultural Industry Technology System Guangxi Innovation Team (Grant No. nycytxgxcxtd-14-06).

Conflict of interest

The authors declare that the research was conducted in the absence of any commercial or financial relationships that could be construed as a potential conflict of interest.

Publisher's note

Supplementary material

The Supplementary Material for this article can be found online at: https://www.frontiersin.org/articles/10.3389/fmars.2022.971648/full#supplementary-material

References

Abehsera, S., Bentov, S., Li, X., Weil, S., Manor, R., Sagi, S., et al. (2021). Genes encoding putative bicarbonate transporters as a missing molecular link between molt and mineralization in crustaceans. *Sci. Rep.* 11 (1), 11722. doi: 10.1038/s41598-021-91155-w

Abehsera, S., Zaccai, S., Mittelman, B., Glazer, L., Weil, S., Khalaila, I., et al. (2018). CPAP3 proteins in the mineralized cuticle of a decapod crustacean. *Sci. Rep.* 8 (1), 2430. doi: 10.1038/s41598-018-20835-x

An, S., Dong, S., Wang, Q., Li, S., Gilbert, L. I., Stanley, D., et al. (2012). Insect neuropeptide bursicon homodimers induce innate immune and stress genes during molting by activating the NF-κB transcription factor relish. *PloS One* 7 (3), e34510. doi: 10.1371/journal.pone.0034510

Bartel, D. (2004). MicroRNAs: Genomics, biogenesis, mechanism, and function. *Cell* 116, 281–297. doi: 10.1016/S0092-8674(04)00045-5

Buhler, K., Clements, J., Winant, M., Vulsteke, V., and Callaerts, P. (2018). Growth control through regulation of insulin signalling by nutrition-activated steroid hormone in Drosophila. *Development* 145(21), dev165654. doi: 10.1242/dev.165654

Cerenius, L., and Söderhäll, K. (2004). The prophenoloxidase-activating system in invertebrates. *Immunol. Rev.* 198, 116–126. doi: 10.1111/j.0105-2896.2004.00116.x

Chang, E. S., and Mykles, D. L. (2011). Regulation of crustacean molting: A review and our perspectives. *Gen. Comp. Endocrinol.* 172 (3), 323–330. doi: 10.1016/j.ygcen.2011.04.003

Chen, Y., Aweya, J. J., Sun, W., Wei, X., Gong, Y., Ma, H., et al. (2018). SpToll1 and SpToll2 modulate the expression of antimicrobial peptides in Scylla paramamosain. *Dev. Comp. Immunol.* 87, 124–136. doi: 10.1016/j.dci.2018.06.008

Chen, X., and Fu, J. (2021). The microRNA miR-14 regulates egg-laying by targeting EcR in honeybees (*Apis mellifera*). *Insects* 12 (4), 351. doi: 10.3390/insects12040351

Gong, Y., Kong, T., Ren, X., Chen, J., Lin, S., Zhang, Y., et al. (2020). Exosome-mediated apoptosis pathway during WSSV infection in crustacean mud crab. *PloS Pathog.* 16 (5), e1008366. doi: 10.1371/journal.ppat.1008366

Gong, Y., Wei, X., Sun, W., Ren, X., Chen, J., Aweya, J. J., et al. (2021). Exosomal miR-224 contributes to hemolymph microbiota homeostasis during bacterial infection in crustacean. *PloS Pathog.* 17 (8), e1009837. doi: 10.1371/journal.ppat.1009837

Gong, J., Ye, H., Xie, Y., Yang, Y., Huang, H., Li, S., et al. (2015). Ecdysone receptor in the mud crab *Scylla paramamosain*: A possible role in promoting ovarian development. *J. Endocrinol.* 224 (3), 273–287. doi: 10.1530/joe-14-0526

González, M., Betancourt, J. L., Rodríguez-Ramos, T., Estrada, M. P., Carpio, Y., and Ramos, L. (2020). Induction of spawning in pacific white shrimp *Litopenaeus vannamei* (Boone 1931) by injection of its molt inhibiting hormone isoform II produced in *E.coli*. *Aquaculture Res.* 51 (8), 31003108. doi: 10.1111/are.14644

Jiang, J., Ge, X., Li, Z., Wang, Y., Song, Q., Stanley, D. W., et al. (2013). MicroRNA-281 regulates the expression of ecdysone receptor (EcR) isoform b in the silkworm, *Bombyx mori*. *Insect Biochem. Mol. Biol.* 43 (8), 692–700. doi: 10.1016/j.ibmb.2013.05.002

Kalluri, R., and LeBleu, V. S. (2020). The biology, function, and biomedical applications of exosomes. *Science* 367 (6478), aau6478. doi: 10.1126/science.aau6977

Lai, Y., Jin, Q., and Zhu, F. (2020). Differential expression of microRNAs in mud crab Scylla paramamosain in response to white spot syndrome virus (WSSV) infection. *Fish shellfish Immunol.* 105, 1–7. doi: 10.1016/j.fsi.2020.06.055

Lemaitre, B., and Hoffmann, J. (2007). The host defense of drosophila melanogaster. *Annu. Rev. Immunol.* 25, 697–743. doi: 10.1146/annurev.immunol.25.022106.141615

Li, J., Sun, J., Dong, X., Geng, X., and Qiu, G. (2019). Transcriptomic analysis of gills provides insights into the molecular basis of molting in Chinese mitten crab (*Eriocheir sinensis*). *PeerJ* 7, e7182. doi: 10.7717/peerj.7182

Liu, L., Fu, Y., Xiao, L., Liu, X., Fang, W., and Wang, C. (2021). iTRAQ-based quantitative proteomic analysis of the hepatopancreas in *Scylla paramamosain* during the molting cycle. *Comp. Biochem. Physiol. Part D Genomics Proteomics* 40, 100870. doi: 10.1016/j.cbd.2021.100870

Liu, N., Landreh, M., Cao, K., Abe, M., Hendriks, G. J., Kennerdell, J. R., et al. (2012). The microRNA miR-34 modulates ageing and neurodegeneration in drosophila. *Nature* 482 (7386), 519–523. doi: 10.1038/nature10810

Lv, J., Zhang, L., Liu, P., and Li, J. (2017). Transcriptomic variation of eyestalk reveals the genes and biological processes associated with molting in *Portunus trituberculatus*. *PloS One* 12 (4), e0175315. doi: 10.1371/journal.pone.0175315

Minh Nhut, T., Mykles, D. L., Elizur, A., and Ventura, T. (2020). Ecdysis triggering hormone modulates molt behaviour in the redclaw crayfish *Cherax quadricarinatus*, providing a mechanistic evidence for conserved function in molt regulation across pancrustacea. *Gen. Comp. Endocrinol.* 298, 113556. doi: 10.1016/j.ygcen.2020.113556

Mykles, D. L. (2021). Signaling pathways that regulate the crustacean molting gland. *Front. Endocrinol. (Lausanne)* 12. doi: 10.3389/fendo.2021.674711

Rekha, R., Vaseeharan, B., Ishwarya, R., Anjugam, M., Alharbi, N. S., Kadaikunnan, S., et al. (2018). Searching for crab-borne antimicrobial peptides: Crustin from portunus pelagicus triggers biofilm inhibition and immune responses of artemia salina against GFP tagged vibrio parahaemolyticus Dahv2. *Mol. Immunol.* 101, 396–408. doi: 10.1016/j.molimm.2018.07.024

Saliminejad, K., Khorram Khorshid, H. R., Soleymani Fard, S., and Ghaffari, S. H. (2019). An overview of microRNAs: Biology, functions, therapeutics, and analysis methods. *J. Cell Physiol.* 234 (5), 5451–5465. doi: 10.1002/jcp.27486

Song, Y., Villeneuve, D. L., Toyota, K., Iguchi, T., and Tollefsen, K. E. (2017). Ecdysone receptor agonism leading to lethal molting disruption in arthropods: Review and adverse outcome pathway development. *Environ. Sci. Technol.* 51 (8), 4142–4157. doi: 10.1021/acs.est.7b00480

Song, J., and Zhou, S. (2020). Post-transcriptional regulation of insect metamorphosis and oogenesis. *Cell Mol. Life Sci.* 77 (10), 1893–1909. doi: 10.1007/s00018-019-03361-5

Sruthy, K. S., and Philip, R. (2021). Anti-lipopolysaccharide factor from crucifix crab *Charybdis feriatus*, cf-ALF2: Molecular cloning and functional characterization of the recombinant peptide. *Probiotics Antimicrob. Proteins* 13 (3), 885–898. doi: 10.1007/s12602-020-09716-w

Strus, J., Znidaršič, N., Blejec, A., and Tušek-Žnidarič, M. (2015). Crustacean cuticle: Synthesis and remodeling of a dynamic extracellular matrix during molt cycle. *Microscopy Microanalysis* 21 (S3), 895–896. doi: 10.1017/S143192715005279

Su, S., Munganga, B. P., Tian, C., Li, J., Yu, F., Li, H., et al. (2021). Comparative analysis of the intermolt and postmolt hepatopancreas transcriptomes provides insight into the mechanisms of *Procambarus clarkii* molting process. *Life (Basel)* 11 (6), 480. doi: 10.3390/life11060480

Sun, G., Zhu, J., and Raikhel, A. S. (2004). The early gene E74B isoform is a transcriptional activator of the ecdysteroid regulatory hierarchy in mosquito vitellogenesis. *Mol. Cell Endocrinol.* 218 (1-2), 95–105. doi: 10.1016/j.mce.2003.12.014

Tanaka, S., Nakamura, T., Morita, T., and Iwanaga, S. (1982). Limulus anti-LPS factor: an anticoagulant which inhibits the endotoxin mediated activation of limulus coagulation system. *Biochem. Biophys. Res. Commun.* 105 (2), 717–723. doi: 10.1016/0006-291x(82)91493-0

Tian, Z., and Jiao, C. (2019). Molt-dependent transcriptome analysis of claw muscles in Chinese mitten crab *Eriocheir sinensis*. *Genes Genomics* 41 (5), 515–528. doi: 10.1007/s13258-019-00787-w

Vay, L. L. (2001). Ecology and management of mud crab Scylla spp. *Asian Fish Sci.* 14 (2), 101111. doi: 10.33997/j.afs.2001.14.2.001

Wang, K. J., Huang, W. S., Yang, M., Chen, H. Y., Bo, J., Li, S. J., et al. (2007). A male-specific expression gene, encodes a novel anionic antimicrobial peptide, scygonadin, in *Scylla serrata*. *Mol. Immunol.* 44 (8), 1961–1968. doi: 10.1016/j.molimm.2006.09.036

Wang, H., Wei, H., Tang, L., Lu, J., Mu, C., and Wang, C. (2018). Identification and characterization of miRNAs in the gills of the mud crab (*Scylla paramamosain*) in response to a sudden drop in salinity. *BMC Genomics* 19, 609. doi: 10.1186/s12864-018-4981-6

Xu, Z., Liu, A., Li, S., Wang, G., and Ye, H. (2020). Hepatopancreas immune response during molt cycle in the mud crab, *Scylla paramamosain*. *Sci. Rep.* 10 (1), 13102. doi: 10.1038/s41598-020-70139-2

Xu, W. F., Qiao, K., Huang, S. P., Peng, H., Huang, W. S., Chen, F. Y., et al. (2011). The expression pattern of scygonadin during the ontogenesis of *Scylla paramamosain* predicting its potential role in reproductive immunity. *Dev. Comp. Immunol.* 35 (10), 1078–1090. doi: 10.1016/j.dci.2011.03.028

Yoo, B., Kim, H. Y., Chen, X., Shen, W., Jang, J. S., Stein, S. N., et al. (2021). 20-hydroxyecdysone (20E) signaling regulates amnioserosa morphogenesis during drosophila dorsal closure: EcR modulates gene expression in a complex with the AP-1 subunit, jun. *Biol. Open* 10 (8). doi: 10.1242/bio.058605

Yuan, D., Zhou, S., Liu, S., Li, K., Zhao, H., Long, S., et al. (2020). The AMPK-PP2A axis in insect fat body is activated by 20-hydroxyecdysone to antagonize insulin/IGF signaling and restrict growth rate. *Proc. Natl. Acad. Sci.* 117 (17), 9292–9301. doi: 10.1073/pnas.2000963117

Zhou, Z. K., Gu, W. B., Wang, C., Zhou, Y. L., Tu, D. D., Liu, Z. P., et al. (2018). Seven transcripts from the chitinase gene family of the mud crab *Scylla paramamosain*: Their expression profiles during development and moulting and under environmental stresses. *Aquaculture Res.* 49 (8), 3296–3308. doi: 10.1111/are.13793